

# RESULTS ON CP VIOLATION FROM THE NA48 EXPERIMENT AT CERN

LYDIA ICONOMIDOU-FAYARD

*LAL, Université d'Orsay, bât. 200, 91898 Orsay, France*

ON BEHALF OF THE NA48 COLLABORATION

*NA48 is a Cagliari, Cambridge, CERN, Dubna, Edinburgh, Ferrara, Firenze, Mainz, Orsay, Perugia, Pisa, Saclay, Siegen, Torino, Vienna and Warsaw collaboration*

In this article the current status and latest results of the NA48 experiment at CERN are given. We present in more details the analysis performed for the  $\text{Re}(\varepsilon'/\varepsilon)$  measurement with the combined statistics accumulated during the 1998 and 1999 data periods. Reviewing the NA48 rare decay program, we select to underline the new results on the branching ratio and the  $a_V$  factor for the decay  $K_L \rightarrow \pi^0\gamma\gamma$  and the  $K_L \rightarrow \pi^+\pi^- e^+e^-$  CP violating decay.

## 1 Introduction

### 1.1 The NA48 experiment at CERN

The main goal of NA48 is the precise measurement of  $\text{Re}(\varepsilon'/\varepsilon)$  in the neutral kaon system. In order to achieve an accuracy of  $\sim 2 \times 10^{-4}$  the optimization of the detector and beams has been conceived to allow the minimisation of the sensitivity to systematic effects. Moreover, several data taking periods have been carried out, namely in 97, 98, 99 and 2000, to accumulate adequately large statistics. A first result was published in 1999, based on the data sample recorded during the first year <sup>1</sup>. A second, more precise result, was announced on May 2001, coming out from the combined 98 and 99 data and also exploiting information from the special 2000 run for checking purposes. The corresponding analysis will be presented in this article. During the summer 2001, NA48 records its last sample dedicated to  $\text{Re}(\varepsilon'/\varepsilon)$  measurement with a better beam duty cycle and new drift chambers.

The NA48 trigger bandwidth allows to record in parallel with the  $\text{Re}(\varepsilon'/\varepsilon)$  program, several rare kaon decay channels that we will review here. Some of these decays are interesting for testing Chiral Perturbation theory. Others are related to CP-Violation. Finally, several rare modes can probe extensions of the

Standard Model.

### 1.2 CP Violation in neutral kaons

A small non-conservation of the CP symmetry manifests in the neutral kaon system through the observation of the forbidden decay mode  $K_L \rightarrow 2\pi$ . Shortly after the discovery <sup>2</sup> the standard Model described theoretically the phenomenon <sup>3</sup>: the bulk of CP violation in the kaon system is due to the mixing of CP eigenstates  $K_1$  and  $K_2$ , inside the physical particles  $K_S$  and  $K_L$ :

$$K_S = K_1 + \varepsilon K_2 \quad K_L = K_2 + \varepsilon K_1$$

This main contribution to the CP Violation is called *indirect* and it is indicated by the parameter  $\varepsilon$ . A second weaker but measurable component can arise in the kaon decay process <sup>4</sup>: comparing the size of CP Violation in the  $K_L \rightarrow \pi^+\pi^-$  and  $K_L \rightarrow \pi^0\pi^0$  one measures the strength of this component, called *direct* and represented by the parameter  $\varepsilon'$ . Direct CP violation is expected to be  $\sim 1/1000$  of the indirect component. The ratio  $\text{Re}(\varepsilon'/\varepsilon)$  is only weakly bounded by theory to be between 0 and  $30 \times 10^{-4}$ , essentially because of large uncertainties in the hadronic part of the computation <sup>5</sup>. An experimental measurement of  $\text{Re}(\varepsilon'/\varepsilon)$  accurate to few  $10^{-4}$  becomes therefore necessary to detect direct CP-Violation.

### 1.3 The observables and the NA48 method

The measurable quantity  $\text{Re}(\varepsilon'/\varepsilon)$  is connected to the double ratio  $R$  of four decay rates as follows:

$$R = \frac{\Gamma(K_L \rightarrow \pi^0\pi^0)}{\Gamma(K_S \rightarrow \pi^0\pi^0)} / \frac{\Gamma(K_L \rightarrow \pi^+\pi^-)}{\Gamma(K_S \rightarrow \pi^+\pi^-)} \approx 1 - 6 \times \text{Re}(\varepsilon'/\varepsilon)$$

In experimental conditions this becomes:

$$R_{exp} = \frac{Nb(K_L \rightarrow \pi^0\pi^0)}{Nb(K_S \rightarrow \pi^0\pi^0)} / \frac{Nb(K_L \rightarrow \pi^+\pi^-)}{Nb(K_S \rightarrow \pi^+\pi^-)} \approx 1 - 6 \times \text{Re}(\varepsilon'/\varepsilon)_{exp}$$

where branching ratios have been replaced by the numbers of detected events in each final mode within the acceptance of the experiment. To obtain the true double ratio  $R$  one has to correct the measured  $R_{exp}$  by a factor  $A_{corr}$  which would take into account all acceptance, trigger and analysis effects, such that:

$$R_{true} = R_{exp} + A_{corr} \quad (1)$$

In practice, measuring accurately  $\text{Re}(\varepsilon'/\varepsilon)$  is equivalent to measure accurately the correction factor  $A_{corr}$ . All experimental efforts will concentrate to identify, minimise and precisely quantify all possible sources of biases.

Notice that since  $R$  is a double ratio, a series of effects affecting simultaneously all four decay modes would cancel. This feature is fully exploited in NA48:  $K_L \rightarrow \pi^0\pi^0$ ,  $K_L \rightarrow \pi^+\pi^-$ ,  $K_S \rightarrow \pi^+\pi^-$  and  $K_S \rightarrow \pi^0\pi^0$  are concurrently recorded thanks to the use of two almost parallel beams. This implies that beam flux variations, trigger or detector instabilities affect similarly at least two of the four components and therefore leave the double ratio invariant at first order. Geometrical acceptance doesn't vanish in the double ratio: indeed, because of the very different  $K_L$  and  $K_S$  lifetimes and the no-similar kinematics of  $\pi^+\pi^-$  and  $\pi^0\pi^0$  final modes, this particular correction can reach up to  $\pm 10\%$  on  $R$ , depending on the kaon energy. In order to avoid

a such large contribution to  $A_{corr}$ , the  $K_L$  decay spectrum is weighted to behave like the  $K_S$  one, so that the acceptance correction is minimised.

CP-conserving processes pollute to some extent the two  $K_L$  samples. These are  $K_L \rightarrow \pi e \nu$  and  $K_L \rightarrow \pi \mu \nu$  decays behaving like  $K \rightarrow \pi^+\pi^-$  and  $K_L \rightarrow \pi^0\pi^0\pi^0$  with missing or fused photons and satisfying all selection criteria of  $K_L \rightarrow \pi^0\pi^0$ . Their effect doesn't vanish in the double ratio and has to be carefully studied. Finally, all residual corrections have to be evaluated and combined into  $A_{corr}$ .

## 2 The NA48 Beams

$K_S$  and  $K_L$  beams<sup>6</sup> are both produced by the 450 GeV proton beam delivered by the SPS. An amount of  $\sim 1.5 \times 10^{12}$  protons per pulse hit a first beryllium target located  $\sim 126$  m upstream of the decay volume. The outgoing beam is let flying through long collimation and bending magnets (fig. 1). This distance of  $\sim 126$  m is enough for the  $K_S$  component to almost completely decay, so that at the exit of the final collimator a pure  $K_L$  beam is dominating.

The protons surviving after the  $K_L$  target are deviated and sent to cross a bent crystal<sup>7</sup>. By tuning the incidence angle, one selects the flux of transmitted protons following the crystalline planes to be  $\sim 3 \times 10^7$  per pulse. The bending acts in an only 6 cm length without cancelling the upstream deflection on other charged particles. The transmitted protons pass through a tagging station which measures very precisely the crossing time of all protons. After several deflections this beam is sent to strike a second target, located  $\sim 6$  m before the decay volume and 7.2 cm above the  $K_L$  beam. An outgoing  $K_S$  beam is therefore dominating the decays at the exit of the final collimator. The two,  $K_S$  and  $K_L$ , beam axes are slightly converging in order to intersect at the centre of the

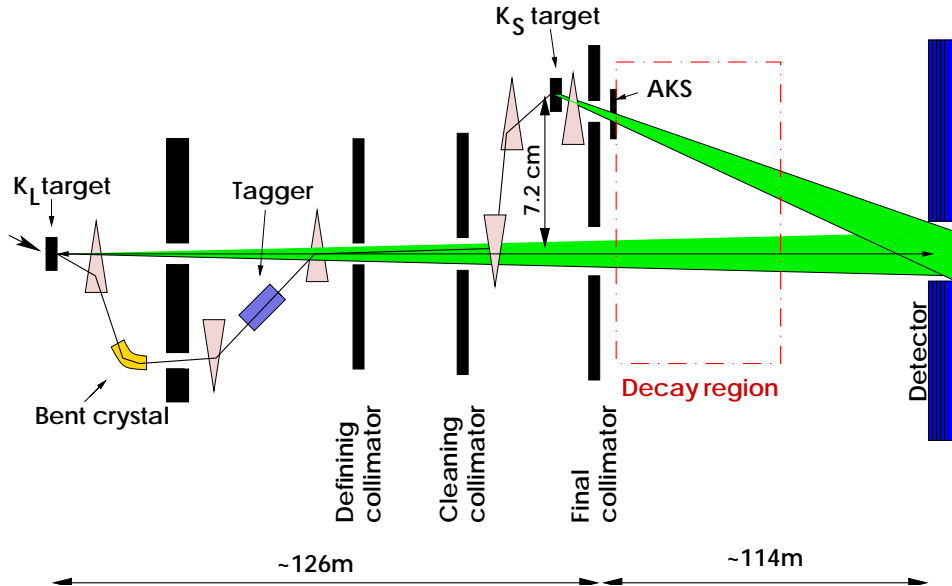


Figure 1. Schematic view of the beam lines.

detector 120 m away and illuminate similarly the sensitive NA48 volume.

Since  $K_S$  and  $K_L$  beams are both produced by the same primary proton beam they undergo the same intensity fluctuations, at first order. Beam extraction from the SPS makes that  $K_S/K_L$  ratio can vary by  $\pm 10\%$  during the burst. Slower variations during the data taking periods can originate from changes in the beam steering. Along the two years the variance of the  $K_S/K_L$  intensity ratio was  $\sim 9\%$ . This ratio is continuously monitored and applied as weighting factor to the data to make the result insensitive to eventual unaccounted detector variations effects.

Beams are tuned such that within the decay volume the kaon energy spectra for  $K_S$  and  $K_L$  decays are similar to  $\pm 15\%$  in the energy range used in the analysis, namely from 70 to 170 GeV.

### 3 The Detector

The NA48 detector is designed to precisely identify and reject the CP-conserving component of the  $K_L$  decays and to be able to

register high rates for long periods in stable conditions.

Charged particles are measured by a magnetic spectrometer housed in a tank filled with helium. Two drift chambers are located before and two after the central dipole magnet which produce an integrated magnetic field of 0.88 Tm. This corresponds to a transverse momentum kick of 265 MeV/c. Each chamber<sup>8</sup> consists of eight wire planes oriented following four directions, X, Y, U and V. This allows to solve reconstruction ambiguities and to have sufficient redundancy in case of wire inefficiencies. The momentum resolution is  $\sigma(p)/p = 0.48\% \oplus 0.009 \times p\%$  where p is in GeV/c. The kaon mass is reconstructed in  $\pi^+\pi^-$  decays with a resolution of 2.5 MeV.

Neutral decays are measured by the LKr calorimeter<sup>9</sup>. This is a quasi-homogeneous device consisting of  $\sim 10 m^3$  of liquid Krypton and of readout electrodes, made of  $50 \mu m \times 18 mm \times 125 cm$  Cu-Be-Co ribbons pulled in longitudinal projective towers pointing to the centre of the decay region. A cell is defined by an anode in between two

cathodes, such that the calorimeter is segmented in  $\sim 13000$  cells of  $2 \times 2$  cm<sup>2</sup> section. The initial current readout technique reinforces the uniformity of the energy response and provides high rate capability. Cell-to-cell response is equalised down to 0.15% by comparing the cluster energy to the momentum measured by the spectrometer of electrons from  $K_L \rightarrow \pi e \nu$  decays. The pure calorimeter resolution is found to be:

$$\frac{\sigma(E)}{E} = \frac{(3.2 \pm 0.2)\%}{\sqrt{E}} \oplus \frac{(9 \pm 1)\%}{E} \oplus (0.42 \pm 0.05)\%$$

After all corrections the energy response is linear within 0.1%. The position of a cluster is reconstructed with a resolution of 1mm in both directions.

The tagger station <sup>10</sup> is made of two ladders of scintillator fingers, crossing the beam horizontally and vertically. Counter widths are decreasing from 3.0 mm at the edges to 0.2 mm in the center of the ladder, following the beam profile in order to equalise the counting rates. A small overlap between two adjacent counters guarantees the complete coverage of the beam. A proton crossing the tagging station is measured by at least two counters, one in the horizontal and one in the vertical ladder. The reconstructed time per counter is known to  $\sim 140$  ps and the separation of two close protons is effective down to 4-5 ns.

At the exit of the final collimator an anti-counter <sup>11</sup> vetoes all upstream decays of the  $K_S$  beam (AKS). Its sharp edge gives the geometrical reference used for checking the stability of the energy scale.

An hadronic calorimeter following the LKr offers energy measurement contributing to the trigger. A series of muon counters provide time information to identify  $K_L \rightarrow \pi \mu \nu$  decays.

## 4 The analysis

The data analysis for the  $\text{Re}(\varepsilon'/\varepsilon)$  measurement is done in the following steps:

1.  $\pi^+ \pi^-$  and  $\pi^0 \pi^0$  decays are reconstructed
2. These two samples are then identified as originated from the  $K_S$  or the  $K_L$  beam, using the tagging information
3. The remaining 3-body background is subtracted from the  $K_L$  sample in both  $\pi^+ \pi^-$  and  $\pi^0 \pi^0$  modes
4. Corrections are applied and the corresponding systematic uncertainties are evaluated
5. The double ratio is computed and its stability with respect to several variables is checked

### 4.1 $\pi^+ \pi^-$ and $\pi^0 \pi^0$ reconstruction

Charged decays are reconstructed using the hits found in the drift chambers. Hits are combined to tracks. Tracks found in the two chambers before the magnet are extrapolated back and the decay vertex is defined as their closest distance of approach in space. The kaon energy is computed from the opening angle between the two tracks before the magnet and the ratio of two pions momenta. This method makes the measurement independent from momentum scale uncertainties. Only the distance scale is sensitive to the geometry differences between the two first chambers and also on their relative distance, contributing to the double ratio by  $(2.0 \pm 2.8) \times 10^{-4}$ . Time information for the decay is provided by the scintillator hodoscope with a precision of  $\sim 140$  ps.

Neutral decays are reconstructed from energies and positions of the photons measured by the calorimeter. The assumption that the invariant mass of the four photons is the kaon mass allows to reconstruct the longitudinal coordinate of the vertex. Then

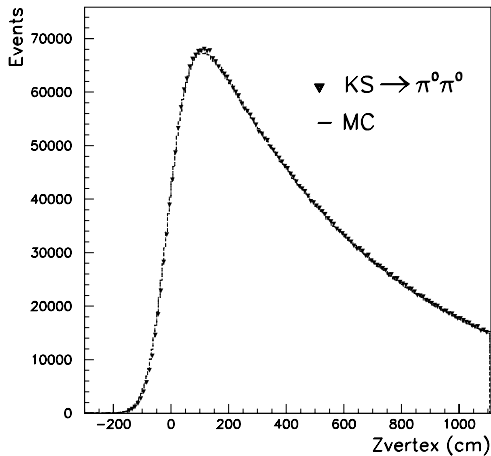


Figure 2. Distribution of the reconstructed vertex position of  $K_S \rightarrow \pi^0 \pi^0$  candidates. The nominal AKS position is at  $Z_{vertex}=0$

combining the four showers to photon pairs one chooses the two closest to the nominal  $\pi^0$  mass. This fully reconstructs the  $K \rightarrow \pi^0 \pi^0$  final modes while in case of  $K_L \rightarrow \pi^0 \pi^0 \pi^0$  with missing photons no resonant  $\gamma - \gamma$  mass is found. The calorimeter provides very precise time information for the decay. A combination of the four photon times gives the event time with an accuracy of  $\sim 220$  ps.

The decay volume is determined such that the sensitivity of the result on uncertainties -essentially related to the neutral energy scale and acceptance- are minimised. Events are accepted if the kaon energy belongs to the range from 70 to 170 GeV and if their longitudinal decay vertex position is no more than 3.5 times the  $K_S$  lifetime starting from the  $K_S$  anti-counter position. The use of a common decay volume implies that the energy and lifetime definition should be the same for  $\pi^+ \pi^-$  and  $\pi^0 \pi^0$  decays. In charged decays the scale is given by the geometry of the two first chambers as quoted above. In neutral decays, the LKr information defines both energy and vertex scales. To

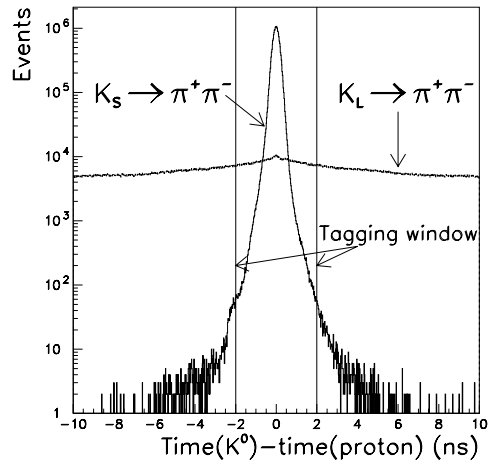


Figure 3. Distribution of the event time minus the closest proton time for  $K_S \rightarrow \pi^+ \pi^-$  and  $K_L \rightarrow \pi^+ \pi^-$  events identified from their vertex position in the vertical plane

control the correctness and stability of the energy scale we compare the reconstructed position of the sharp AKS edge to its nominal value (figure 2). Any deviation is corrected by a global factor applied to the response of all channels. Uncertainties on the energy reconstruction are deeply studied and are related to energy leakage between close showers, non-linearities, residual energy and transverse scales and non gaussian tails<sup>12</sup>. The total effect on the double ratio leads to an uncertainty of  $\pm 5.8 \times 10^{-4}$ .

#### 4.2 Distinguishing a $K_S$ from a $K_L$

An event will be classified as coming from the  $K_S$  beam if a proton is found in the tagger within  $\pm 2$  ns. Figure 3 shows the distribution of the event time minus its closest proton time for  $K_S \rightarrow \pi^+ \pi^-$  and  $K_L \rightarrow \pi^+ \pi^-$  identified as such from their vertex position in the vertical plane.

In case of true  $K_S$  decays, almost all events have a proton in coincidence within

$\pm 2$  ns. The small fraction of events lying outside the tagging window corresponds to time reconstruction inefficiencies and it is called  $\alpha_{SL}$ . This will cause  $K_S$  decays to be mislabelled  $K_L$  and it must be corrected in the result. On the other hand, because of the high counting rate in the tagging station,  $K_L$  decays can accidentally have a time coincidence with a proton. The result must therefore be corrected for the fraction of  $K_L$  decays (called  $\alpha_{LS}$ ) mis-accounted as  $K_S$ . In addition the double ratio is particularly sensitive to eventual differences of  $\alpha_{LS}$  and  $\alpha_{SL}$  between  $\pi^+\pi^-$  and  $\pi^0\pi^0$  modes. Tagging mis-identification factors require therefore a precise measurement in both modes.

$K_S \rightarrow \pi^+\pi^-$  decays recognised by their vertex position allow the study of *tagging inefficiency*  $\alpha_{SL}$ . The fraction of  $(1.63 \pm 0.03) \times 10^{-4}$  of events having the closest proton time further than 2 ns (see figure 3) have been scrutinized and found to be due in  $\sim 80\%$  of cases to mis-reconstruction of the proton time. This is therefore symmetrically affecting  $\pi^+\pi^-$  and  $\pi^0\pi^0$  such that the double ratio remains invariant. However an eventual efficiency difference of the event time reconstruction has to be considered between the hodoscope and the LKr calorimeter, providing information for  $\pi^+\pi^-$  and  $\pi^0\pi^0$  events respectively. This is studied looking at  $K \rightarrow \pi^0\pi^0$  and  $K_L \rightarrow \pi^0\pi^0\pi^0$  events with a photon conversion. The two electron tracks allow the time reconstruction from the hodoscope while the photons contained in the event give the decay time information from the calorimeter. The number of cases where these two time estimators differ by more than 2 ns corresponds to the differential inefficiency between the hodoscope and the calorimeter. This method allows to show that  $\alpha_{SL}$  is identical for  $K_S \rightarrow \pi^+\pi^-$  and  $K_S \rightarrow \pi^0\pi^0$  with an uncertainty of  $\pm 0.5 \times 10^{-4}$ . This translates to  $\pm 3 \times 10^{-4}$  uncertainty on the double ratio. This result has been crosschecked and con-

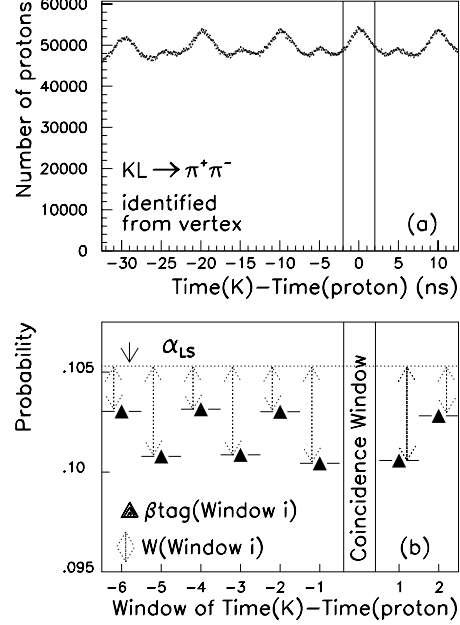


Figure 4. In (a) distribution of proton times with respect to event time for  $K_L \rightarrow \pi^+\pi^-$  events identified from their vertex. In (b) variables  $\alpha_{LS}$ ,  $\beta_{tag}$  and  $W$  are schematically shown for tagged  $K_L$  events.

firmed with  $\pi^0\pi^0$  data recorded with a single  $K_S$  beam and also with  $K \rightarrow \pi^0\pi^0$  events with a subsequent Dalitz decay, where the track vertex reconstruction in the vertical plane provides the beam origin.

We call *dilution* the fraction  $\alpha_{LS}$  of  $K_L$  events misidentified as  $K_S$  because of an accidental coincidence with a proton. This only depends on the proton rate in the tagger and must equally affect both decay modes.  $K_L \rightarrow \pi^+\pi^-$  events recognised by their vertex allow to measure  $\alpha_{LS} = (10.649 \pm 0.008)\%$  (see figure 4.a). A direct evaluation of  $\alpha_{LS}$  in  $K_L \rightarrow \pi^0\pi^0$  decays is not possible. We use, instead of the coincidence window, out-of-time windows, 4 ns wide, in events tagged as  $K_L$ . This is done for both  $K_L \rightarrow \pi^+\pi^-$  and  $K_L \rightarrow \pi^0\pi^0$  events, using several such windows to increase the statistical accuracy. Because  $K_L$  tagged events do not have any proton in coincidence, the dilution  $\beta_{tag}$  measured in lateral windows is smaller than

$\alpha_{LS}$  by a quantity  $W$  (see figure 4.b).  $W^{+-}$  is measured directly in  $\pi^+\pi^-$  using  $K_L \rightarrow \pi^+\pi^-$  identified from vertex. For  $W^{00}$  we use  $K_L \rightarrow \pi^0\pi^0\pi^0$  events assuming that their tagging properties are identical to those of the  $K_L \rightarrow \pi^0\pi^0$  sample. We exploited a special  $K_L$  run taken in 2000 to confirm this hypothesis. Combining all the available information we found that:

$$\begin{aligned}\Delta\alpha_{LS} &= \alpha_{LS}^{00} - \alpha_{LS}^{+-} \\ &= (\beta_{LS}^{00} + W^{00}) - (\beta_{LS}^{+-} + W^{+-}) \\ &= (4.3 \pm 1.8) \times 10^{-4}\end{aligned}$$

This difference indicates that  $\pi^0\pi^0$  events are recorded in slightly higher intensity conditions than  $\pi^+\pi^-$ . This has been quantitatively explained by the higher sensitivity of the charged events to the accidental activity at both trigger and reconstruction levels. From these two contributions one would expect  $\Delta\alpha_{LS} = (3.5 \pm 0.5) \times 10^{-4}$  in good agreement with the measurement.  $\Delta\alpha_{LS}$  implies a correction on the double ratio of  $+(8.3 \pm 3.4) \times 10^{-4}$ .

#### 4.3 Background subtraction

$K_L$  events contain a fraction of the 3-body decays, highly suppressed by trigger conditions and analysis cuts. In charged mode case,  $K_L \rightarrow \pi\mu\nu$  and  $K_L \rightarrow \pi e\nu$  events can mimic good  $\pi^+\pi^-$  decays if the electron or the muon is not recognised by the E/p variable or the muon vetoes respectively. Because of the undetected neutrino of these 3-body modes the missing transverse momentum of the decay,  $P_T'^2$ , is larger than in a  $\pi^+\pi^-$  event (see figure 5). Moreover the reconstructed 2-track invariant mass follows different distributions than in  $\pi^+\pi^-$ . Studying the correlation of  $P_T'^2$  versus  $M_{\pi^+\pi^-}$  in different control regions for  $\pi^+\pi^-$ ,  $K_L \rightarrow \pi\mu\nu$  et  $K_L \rightarrow \pi e\nu$  identified samples, allows to determine the contamination of the signal region.

We found that the  $K_L \rightarrow \pi^+\pi^-$  sample contains after all cuts  $16.3 \times 10^{-4}$  of 3-body residual background, dominated by

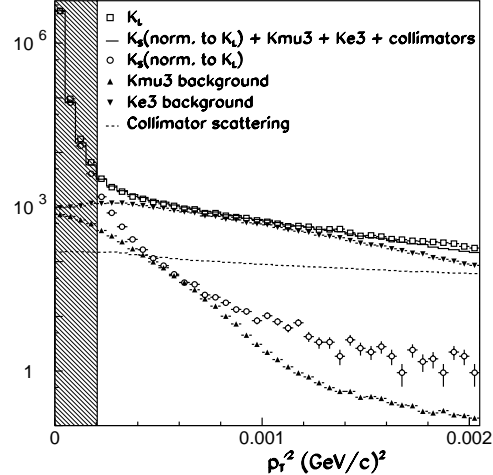


Figure 5. Distribution of transverse momentum  $P_T'^2$  and comparison of the data with all known components. The signal region is defined for  $P_T'^2 < 0.0002 GeV/c^2$

$K_L \rightarrow \pi e\nu$ . The corresponding correction on the double ratio is  $(16.8 \pm 3.0) \times 10^{-4}$  where the error takes also into account systematic variations related to the control region choices. Notice that  $P_T'^2$  is the component of the transverse momentum which is orthogonal to the kaon line of flight, reconstructed in DCH1 and assumed to come from the target. The advantage of this definition is to equalise the distributions for  $K_S$  and  $K_L$  decays despite the very different positions of the corresponding targets. Only a small asymmetry of  $\leq 2 \times 10^{-4}$  remains between the two beams because of no gaussian tail effects.

When  $K_L \rightarrow \pi^0\pi^0\pi^0$  events have two photons either escaping acceptance or fused, the two reconstructed invariant  $\gamma - \gamma$  masses do not agree with the nominal  $\pi^0$  one. This is observed looking at a  $\chi^2$  variable testing this compatibility as shown in figure 6. In  $K_L \rightarrow \pi^0\pi^0$  candidates an excess of events is observed for high values of  $\chi^2$  with respect to  $K_S \rightarrow \pi^0\pi^0$ , where the existing tail corresponds to events with converted photons or with hadronic photoproduction. The amount

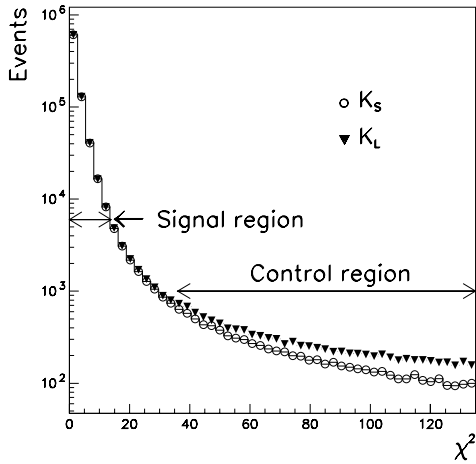


Figure 6. The  $\chi^2$  distribution for tagged  $K_L \rightarrow \pi^0\pi^0$  and  $K_S \rightarrow \pi^0\pi^0$  candidates

of remaining background in  $K_L \rightarrow \pi^0\pi^0$  is checked in a control region, properly subtracting the normalised  $K_S$  from the  $K_L$  integrated population. The extrapolated fraction of 3-body pollution under the  $\pi^0\pi^0$  signal results to a correction on the double ratio of  $(-5.9 \pm 2.0) \times 10^{-4}$ .

$K_S$  beam is free from physical background. The  $\Lambda \rightarrow p\pi^-$  decays are eliminated down to  $\leq 10^{-4}$  level, by a track momentum asymmetry cut applied to both beams.

Kaon scattering in the inner edges of the collimators may modify the kinematics of an event. In  $K_S$  beam, scattering may happen at the level at the final collimator and also when kaons cross the anticounter. In both cases, the transverse momentum of the event is enhanced. After all cuts, the amount of scattered events in the final sample is almost identical in  $\pi^+\pi^-$  and  $\pi^0\pi^0$  modes: the halos of centre of gravity distributions, populated by the halo of the beam and the scattered events, are very similar, as shown in figure 7.a. In  $K_L$  case, kaons or accompanying neutrons in the halo of the beam can scatter

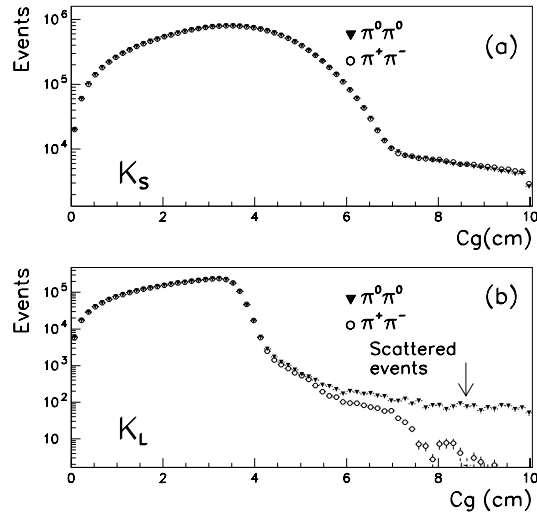


Figure 7. Centre of gravity distributions for  $K_S$  and  $K_L$  events after all cuts.

or double-scatter in the aperture of the collimators, producing in some cases a  $K_S$  component.  $K_S$  particle decays are indeed observed in  $K_L$  beam at high transverse momenta accumulating around the kaon invariant mass: they all originate from the lips of the two last collimators and they decay with the  $K_S$  lifetime. These scattered events are asymmetrically rejected in  $\pi^+\pi^-$  and  $\pi^0\pi^0$  modes as indicated by the different halos of the centre of gravity distributions (figure 7.b). The corresponding correction is computed to be  $(-9.6 \pm 2.0) \times 10^{-4}$  on the double ratio.

#### 4.4 Double ratio, corrections and systematics

After all cuts, tagging and background corrections we obtained for the combined 98+99 data periods a statistics of 3.29M of  $K_L \rightarrow \pi^0\pi^0$ , 5.21M of  $K_L \rightarrow \pi^+\pi^-$ , 14.45M of  $K_S \rightarrow \pi^0\pi^0$  and 22.22M of  $K_S \rightarrow \pi^+\pi^-$  decays. Before combining these four samples to obtain the double ratio one



has to apply some corrections. The method of the double ratio and the simultaneous data taking of the four modes implies that most of the effects cancel in the result at first order. Eventual differential effects can survive and have to be considered. Such are for instance the tagging corrections presented in 4.2. Another effect concerns trigger inefficiencies. In charged mode,  $\sim 2\%$  of the events are lost at the trigger level essentially because of wire inefficiencies and of information spoiled in presence of accidentals. This amount is identical between  $K_S$  and  $K_L$  down to  $(-3.6 \pm 5.2) \times 10^{-4}$ . The neutral trigger is efficient to  $99.920 \pm 0.009\%$  level with no measurable  $K_S - K_L$  difference. Dead times are applied commonly in all four modes in order to guarantee cancellation and identical intensity conditions.

The high rates of the  $K_L$  beam makes occasionally possible the mismeasurement of a good event because of additional activity. This may create losses of good events. The high correlation of beam variations between  $K_S$  and  $K_L$  together with the concurrent data taking lead to no observable bias on the double ratio due to accidental losses within a  $\pm 4.2 \times 10^{-4}$  uncertainty.

A no cancelling effect in the double ratio is the acceptance correction.  $K_S$  and  $K_L$  acceptances are not identical because of the very different corresponding lifetimes. To avoid a correction on R as large as  $\pm 10\%$  depending on the kaon energy, we choose to weight the  $K_L$  decay spectrum by the ratio between  $K_S$  and  $K_L$  decay intensities into  $\pi\pi$  taking into account the interference term as well. This procedure makes by definition the detector to be illuminated similarly by the two beams. A small residual effect is due to the 0.6 mrad convergence angle between  $K_S$  and  $K_L$  beam lines, causing an acceptance difference in  $\pi^+\pi^-$  events essentially in the first chamber around the beam pipe (see figure 8). This is evaluated using a large statistics Monte Carlo simulating the two

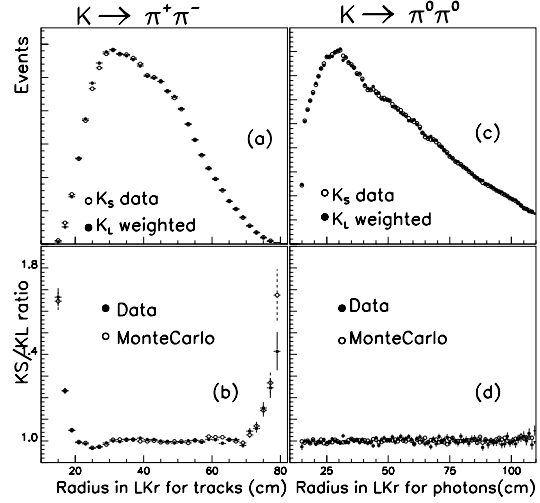


Figure 8. Illumination of the calorimeter by  $\pi^+\pi^-$  tracks for  $K_S$  and weighted  $K_L$  events in (a). The  $K_S/K_L$  ratio is shown in (b) where the residual effect around the beam pipe is seen. In neutral mode  $K_S$  and weighted  $K_L$  decays illuminate similarly the calorimeter (shown in c and d). The distributions are shown for events in a kaon energy range from 95-100 GeV

beams and detector geometry, parametrising particle interactions and using a photon shower library generated by GEANT. The correction on the double ratio is found to be  $(+26.7 \pm 4.1(\text{stat}) \pm 4.0(\text{syst})) \times 10^{-4}$ . The systematic error accounts for uncertainties on beam halo variations, beam shapes, particle interactions in charged mode and wire inefficiencies.

In table 1 we give all corrections applied to the double ratio  $R_{exp}$  and their uncertainties. The double ratio is corrected by  $A_{corr} = (35.9 \pm 12.6) \times 10^{-4}$ , the biggest effects coming from acceptance, charged background, scattering and tagging. The quoted errors account for both statistical and systematic uncertainties and in some cases are still statistically limited.

The double ratio is computed in 20 bins of 5 GeV in kaon energy in order to further decrease the effect of the remaining energy spectra difference between  $K_L$  and  $K_S$ . All

Table 1. Table of corrections applied to the double ratio with their uncertainties

	in $10^{-4}$
Trigger inefficiency in $\pi^+\pi^-$	-3.6 $\pm$ 5.2
AKS inefficiency	+1.1 $\pm$ 0.4
Reconstruction effects of $\pi^0\pi^0$	— $\pm$ 5.8
Reconstruction effects of $\pi^+\pi^-$	+2.0 $\pm$ 2.8
Background subtraction to $\pi^0\pi^0$	-5.9 $\pm$ 2.0
Background subtraction to $\pi^+\pi^-$	+16.9 $\pm$ 3.0
Beam scattering in $K_L$	-9.6 $\pm$ 2.0
Accidental tagging	+8.3 $\pm$ 3.4
Tagging inefficiency	— $\pm$ 3.0
Acceptance correction statistical	+26.7 $\pm$ 4.1
Acceptance correction systematic	— $\pm$ 4.0
Accidental activity	— $\pm$ 4.4
Long term intensity variations of $K_S/K_L$	— $\pm$ 0.6
Total $A_{corr}$	+35.9 $\pm$ 12.6

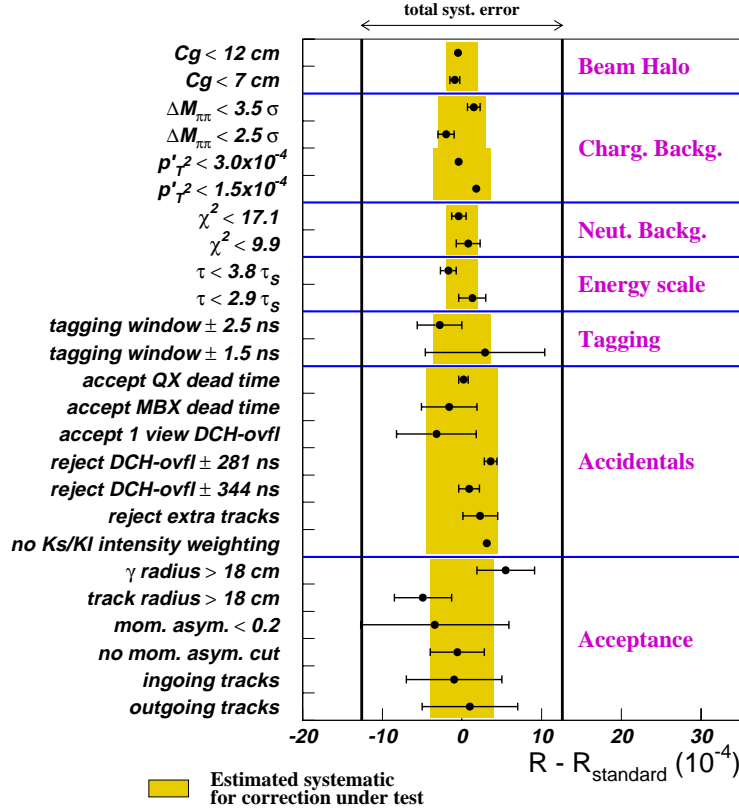


Figure 9. Stability of the double ratio when varying selection criteria

corrections are applied in bins and the 20 values are averaged using an unbiased estimator. The result is:

$$R=0.99098\pm 0.00101(\text{stat})\pm 0.00126(\text{syst})$$

A large number of systematic checks were devoted to verify the stability of the result with a change in the event selection. We cumulate the output of the most important tests in figure 9 where the deviations of the double ratio with respect to its standard value are shown for a series of modifications we did in the procedure. All these checks demonstrated the stability of the result within the allowed systematic range. Moreover, the result was found to be stable with the data taking time, time within the burst, proton revolution phase in the SPS, magnetic field sign in the spectrometer and 50 Hz phase.

The corresponding  $\text{Re}(\varepsilon'/\varepsilon)$  value on 98+99 data<sup>13</sup> is obtained subtracting R from 1 and dividing by six:

$$\text{Re}(\varepsilon'/\varepsilon)=(15.0\pm 1.7(\text{stat})\pm 2.1(\text{syst}))\times 10^{-4}$$

which, combined with the published 97 result gives:

$$\text{Re}(\varepsilon'/\varepsilon)=(15.3\pm 2.6)\times 10^{-4}$$

This result confirms the existence of a direct CP-Violating component in the neutral kaon decays at the level of  $5.9\sigma$ . The 2001 new world average, combining the four most precise experimental results from NA31<sup>14</sup>, E731<sup>15</sup>, KTeV<sup>16</sup> and the combined 97+99+99 NA48 value becomes:

$$\text{Re}(\varepsilon'/\varepsilon)=(17.2\pm 1.8)\times 10^{-4}$$

## 5 Review of the NA48 rare decay program

Several  $K_S$  and  $K_L$  rare decay channels have been looked at in NA48. Table 2 gives a non exhaustive list of observations or limits obtained with NA48 data. We will concentrate here on two results concerning the recently

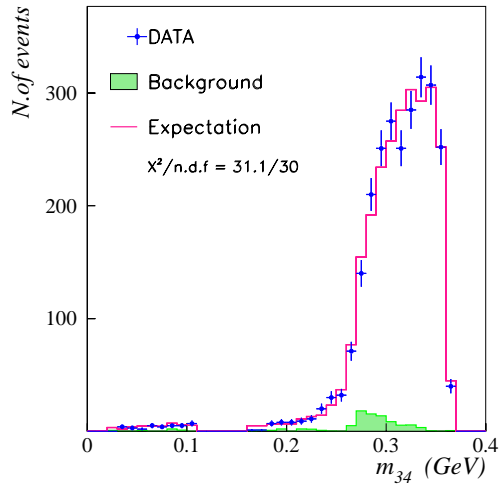


Figure 10. Distribution of the invariant  $\gamma - \gamma$  mass,  $m_{34}$ , of the non resonant photons

updated analysis of  $K_L \rightarrow \pi^0 \gamma \gamma$  and the CP-Violating mode  $K_L \rightarrow \pi^+ \pi^- e^+ e^-$ . More information on rare decays in NA48 can be found in references<sup>17</sup>.

### 5.1 $K_L \rightarrow \pi^0 \gamma \gamma$

The interest of this mode resides in the fact that, in Chiral Perturbation Theory one needs to include  $O(p^6)$  calculations and vector meson contribution to reproduce the observed rate. These two terms account actually for 1/3 of the total amplitude. Moreover the measurement of this decay gives constraints to the CP conserving amplitude contributing to  $K_L \rightarrow \pi^0 e^+ e^-$ , via a two photon intermediate state.

The reconstruction of this mode uses information of the LKr. An event must contain one  $\gamma - \gamma$  pair compatible with  $\pi^0$  mass and a second  $\gamma - \gamma$  pair not compatible. The main background comes from  $K_L \rightarrow \pi^0 \pi^0$  and  $K_L \rightarrow \pi^0 \pi^0 \pi^0$  decays.  $K_L \rightarrow \pi^0 \pi^0$  with a photon conversion before the magnet destroys the  $\pi^0$  reconstruction. These cases are rejected requiring no hits in the first three drift chambers.  $K_L \rightarrow \pi^0 \pi^0 \pi^0$  decaying in-

Table 2. List of some of the rare decays results obtained in NA48

Mode	Branching ratio	Events	Status
$K_L \rightarrow \pi^0 \gamma \gamma$	$(1.36 \pm 0.05) \times 10^{-6}$	2588	preliminary
$K_S \rightarrow \pi^0 e^+ e^-$	$< 1.4 \times 10^{-7}$ (90% CL)		published
$K_S \rightarrow \gamma \gamma$	$(2.58 \pm 0.42) \times 10^{-6}$	149	published
$K_S \rightarrow \pi^+ \pi^- e^+ e^-$	$(4.3 \pm 0.4) \times 10^{-5}$	921	preliminary
$K_L \rightarrow \pi^+ \pi^- e^+ e^-$	$(3.1 \pm 0.2) \times 10^{-7}$	1337	preliminary
$K_L \rightarrow e^+ e^- e^+ e^-$	$(3.7 \pm 0.4) \times 10^{-8}$	132	preliminary
$K_L \rightarrow e^+ e^- \gamma$	$(1.06 \pm 0.05) \times 10^{-5}$	6864	published
$K_L \rightarrow e^+ e^- \gamma \gamma$	$(6.3 \pm 0.5) \times 10^{-7}$	492	preliminary

side the collimator can fake the signal. Dedicated variables have been studied to reduce this background to a small level. In total we have a signal of 2588 events found in the 98+99 data sample, with an estimated background of only 3.3%. The distribution of the invariant  $\gamma - \gamma$  mass for the non resonant photon pair is shown in figure 10. The low mass region ( $M_{\gamma\gamma} < 260$  MeV) is particularly sensitive to the amount of vector meson production, represented by the coupling constant  $a_V$ . Fitting our data with a likelihood function including the shape predicted by  $\chi$ PT calculations up to  $O(p^6)$  and for several  $a_V$  values, we found the best  $\chi^2$  for:

$$a_V = -0.46 \pm 0.03(\text{stat}) \pm 0.04(\text{syst+theory})$$

Using this coupling constant we obtain the following branching ratio:

$$\text{BR}(K_L \rightarrow \pi^0 \gamma \gamma) = (1.36 \pm 0.03(\text{stat}) \pm 0.4(\text{syst})) \times 10^{-6}$$

where the systematic error is shared between experimental and theoretical uncertainties. A publication is in preparation.

### 5.2 $K_L \rightarrow \pi^+ \pi^- e^+ e^-$

CP Violation appears in the kaon system through small quantities, namely  $\varepsilon \sim 0.2\%$  and  $\varepsilon' \sim 10^{-6}$ . The  $K_L \rightarrow \pi^+ \pi^- e^+ e^-$  decay demonstrates that  $K_L$  can also exhibit strong CP-violating phenomena. Indeed, this chan-

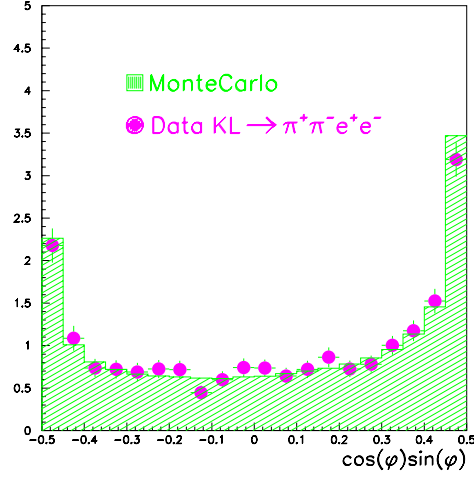


Figure 11.  $\text{Cos}(\phi)\text{sin}(\phi)$  distribution for  $K_L \rightarrow \pi^+ \pi^- e^+ e^-$  decays

nel arises through two diagrams essentially: the inner-bremsstrahlung, violating CP, and the direct emission, CP conserving process. Because the ratio of these two contributions is almost one ( $\sim \eta \times (2M_K/E_\gamma)^2$  where  $E_\gamma$  is the virtual photon energy in the centre of mass), the interference is enhanced. Looking at the angle  $\phi$  between the  $\pi^+ \pi^-$  and  $e^+ e^-$  planes one can observe strong CP asymmetries.

We detected 1337 events after all cuts. The  $\text{cos}(\phi)\text{sin}(\phi)$  distribution is shown in figure 11 where it is also compared with Monte Carlo simulation. After acceptance correc-

tions the measured asymmetry is:

$$A=(13.9\pm 2.7(\text{stat})\pm 2.0(\text{syst}))\%$$

The branching ratio of this decay is found to be:

$$\text{BR}=(3.1\pm 0.1(\text{stat})\pm 0.2(\text{syst}))\times 10^{-7}$$

The measured asymmetry is in agreement with theoretical predictions and previous results<sup>19</sup>. Moreover NA48 detected the first signal of  $K_s \rightarrow \pi^+\pi^-e^+e^-$  decays<sup>20</sup>. This mode conserves CP symmetry. It allows therefore to check eventual effects of final states interactions on the  $\cos(\phi)\sin(\phi)$  distribution, in which case, the  $K_L$  mode would have been also affected. In  $K_S$  beam we measured an asymmetry compatible with zero, based in a sample of 921 events. The observed asymmetry of 13.9% in  $K_L \rightarrow \pi^+\pi^-e^+e^-$  decays is therefore only due to the indirect CP Violation present in this rare process.

### Acknowledgments

It's a pleasure to thank Cecilia Voena, the scientific secretary of the session, for her help. It's amazing how well and happily almost 800 people have lived, worked and have had nice time together in Roma. Thank you profoundly, Juliet, Paolo and the Committee, for the organisation of this excellent conference and please, do it again.

### References

1. V.Fanti et al., Phys. Lett. B465, 335-348 (1999).
2. J.H.Christenson et al., Phys. Lett. 13, 138 (1964).
3. M.Kobayashi and K.Maskawa, Prog. Theor. Phys. 49, 652 (1973).
4. J.Ellis et al., Nucl. Phys. B109, 213 (1976).  
F.J.Gilman and M.B.Wise, Phys. Lett. B83, 83 (1979).
5. S.Bosch et al., Nucl. Phys. B 565, 3 (2000).  
M.Ciuchini et al., hep-ph/9910237  
S.Bertolini et al., Rev. Mod. Phys. 72, 65 (2000)  
E.Pallante, A.Pich, Phys. Rev. Lett. 84, 2568 (2000)  
T.Hambye et al.,Nucl. Phys. B 564, 391 (2000)  
J.Bijnens, J.Prades., hep-ph/0009156  
S.Narison, Nucl. Phys. B 593, 3 (2001)  
See also recent review by M.Ciuchini, Nucl. Phys. B(Proc.Suppl) 99B, 27-34 (2001) and references therein.
6. C.Biino et al., Proc. of 6th EPAC, Stockholm 1998, IOP, 2100-2102 (1999) and CERN-SL-98-033(EA).
7. N.Doble et al., Nucl.Instr. and Methods B 119, 181 (1996).
8. D.Béderède et al., Nucl. Instr. and Methods A 367, 88 (1995).
9. G.D.Barr et al., Nucl. Instr. and Methods A 370, 413 (1993).
10. P.Grafström et al., Nucl. Inst. and Methods A 344, 487 (1994).
11. R.Moore et al., Nucl. Instr. and Methods B 119, 149-155 (1996).
12. G.Unal for the NA48 collaboration, CALOR2000, 9-14 October 2000, Annecy France, hep-ex-0012011.
13. A.Lai et al., CERN-EP/2001-067, hep-ex/0110019, submitted to EPJ.
14. G.Barr et al., Phys. Lett. B 317, 233 (1993).
15. L.K.Gibbons et al., Phys. Rev. Lett. 70, 1203 (1993).
16. See contribution from R.Kessler.
17. E.Mazzucato for the NA48 collaboration, CPconf2000, Nucl. Phys. B (Proc. Suppl) 99B, 81-92 (2001).  
M.Martini for the NA48 collaboration, Proc. of Kaon2001, 12-17 June 2001, Pisa, Italy.  
Publication on  $K_S \rightarrow \pi^0e^+e^-$ , A.Lai et al., Phys. Lett. B514, 253-262 (2001).  
Publication on  $K_S \rightarrow \gamma\gamma$ , A.Lai et al.,

- Phys. Lett. B 493, 29-35 (2000).  
Publication on  $K_L \rightarrow \gamma e^+ e^-$ , V.Fanti et al., Phys. Lett. B 458, 553-563 (1999).
18. G.Ecker et al., Phys. Lett. B 189, 3663 (1987).
  19. P.Heiliger and L.M.Seghal, Phys. Rev. D 48 (1993) 4146; Erratum ibid. D 60 (1999) 079902.  
A.Alavi-Harati et al., Phys. Rev. Lett. 84, 408 (2000).
  20. A.Lai et al., Phys. Lett. B 496, 137-144 (2000).